
Architect of the Bits World: Masked Autoregressive Modeling for Circuit Generation Guided by Truth Table

Haoyuan Wu^{1,2} Haisheng Zheng³ Shoubo Hu² Zhuolun He^{1,4} Bei Yu¹

Abstract

Logic synthesis, a critical stage in electronic design automation (EDA), optimizes gate-level circuits to minimize power consumption and area occupancy in integrated circuits (ICs). Traditional logic synthesis tools rely on human-designed heuristics, often yielding suboptimal results. Although differentiable architecture search (DAS) has shown promise in generating circuits from truth tables, it faces challenges such as high computational complexity, convergence to local optima, and extensive hyperparameter tuning. Consequently, we propose a novel approach integrating conditional generative models with DAS for circuit generation. Our approach first introduces CircuitVQ, a circuit tokenizer trained based on our Circuit AutoEncoder. We then develop CircuitAR, a masked autoregressive model leveraging CircuitVQ as the tokenizer. CircuitAR can generate preliminary circuit structures from truth tables, which guide DAS in producing functionally equivalent circuits. Notably, we observe the scalability and emergent capability in generating complex circuit structures of our CircuitAR models. Extensive experiments also show the superior performance of our method. This research bridges the gap between probabilistic generative models and precise circuit generation, offering a robust solution for logic synthesis.

1. Introduction

With the rapid advancement of technology, the scale of integrated circuits (ICs) has expanded exponentially. This expansion has introduced significant challenges in chip manufacturing, particularly concerning power and area metrics. A primary objective in IC design is achieving the same cir-

cuit function with fewer transistors, thereby reducing power usage and area occupancy.

Logic synthesis (Hachtel & Somenzi, 2005), a critical step in electronic design automation (EDA), transforms behavioral-level circuit designs into optimized gate-level circuits, ultimately yielding the final IC layout. The primary goal of logic synthesis is to identify the physical implementation with the fewest gates for a given circuit function. This task constitutes a challenging NP-hard combinatorial optimization problem. Current logic synthesis tools (Brayton & Mishchenko, 2010; Wolf et al., 2013) rely on human-designed heuristics, often leading to sub-optimal outcomes.

Differentiable architecture search (DAS) techniques (Liu et al., 2018; Chu et al., 2020) offer novel perspectives on addressing challenges in this problem. Circuit functions can be represented through truth tables, which map binary inputs to their corresponding outputs. Truth tables provide a precise representation of input-output relationships, ensuring the design of functionally equivalent circuits. Inspired by this, researchers (Google Deepmind, 2023; Wang et al., 2024) have begun exploring the application of DAS to synthesize circuits directly from truth tables. Specifically, Google Deepmind (2023) proposed CircuitNN, a framework that learns differentiable connection structures with logic gates, enabling the automatic generation of logic circuits from truth tables. This approach significantly reduces the complexity of traditional circuit generation. Building on this, Wang et al. (2024) introduced T-Net, a triangle-shaped variant of CircuitNN, incorporating regularization techniques to enhance the efficiency of DAS.

Despite these advancements, several challenges remain. The computational complexity of DAS grows quadratically with the number of gates, posing scalability issues. Although triangle-shaped architecture (Wang et al., 2024) partially mitigates this problem, redundancy persists. Additionally, DAS is susceptible to converging to local optima (Liu et al., 2018) and hyperparameters (network depth and layer width) require extensive searches. The challenges arise from the vast search space in DAS. Intuitively, limiting the search space through predefined parameters (network depth, gates per layer, and connection probabilities) can significantly reduce the complexity.

¹The Chinese University of Hong Kong, HKSAR ²Noah’s Ark Lab, Huawei, HKSAR ³Shanghai Artificial Intelligent Laboratory, China ⁴ChatEDA Tech, China. Correspondence to: Bei Yu <byu@cse.cuhk.edu.hk>.

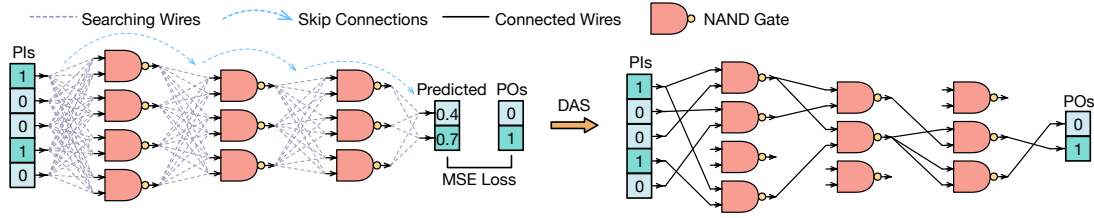


Figure 1. Illustration of differentiable CircuitNN. CircuitNN is designed based on differentiable NAND gates. After DAS is guided by PI and PO pairs of the truth table, CircuitNN can get the precise circuit architecture logic equivalent to the truth table.

Recent advances (OpenAI, 2023; Abramson et al., 2024; Esser et al., 2024; Li et al., 2024a) in conditional generative models have demonstrated remarkable performance across language, vision, and graph generation tasks. Motivated by these developments, we propose a novel approach to circuit generation that generates preliminary circuit structures to guide DAS in generating refined circuits matching specified truth tables. Firstly, we introduce CircuitVQ, a tokenizer with a discrete codebook for circuit tokenization. Built upon our Circuit AutoEncoder framework (Hou et al., 2022; Li et al., 2023a; Wu et al., 2025), CircuitVQ is trained through a circuit reconstruction task. Specifically, the CircuitVQ encoder encodes input circuits into discrete tokens using a learnable codebook, while the decoder reconstructs the circuit adjacency matrix based on these tokens. Subsequently, the CircuitVQ encoder serves as a circuit tokenizer for CircuitAR pretraining, which employs a masked autoregressive modeling paradigm (Chang et al., 2022; Li et al., 2023b). In this process, the discrete codes function as supervision signals. After training, CircuitAR can generate discrete tokens progressively, which can be decoded into initial circuit structures by the decoder of the CircuitVQ. These prior insights can guide DAS in producing refined circuits that match the target truth tables precisely.

Our key contributions can be summarized as follows:

- We introduce CircuitVQ, a circuit tokenizer that facilitates graph autoregressive modeling for circuit generation, based on our Circuit AutoEncoder framework;
- Develop CircuitAR, a model trained using masked autoregressive modeling, which generates initial circuit structures conditioned on given truth tables;
- Propose a refinement framework that integrates differentiable architecture search to produce functionally equivalent circuits guided by target truth tables;
- Comprehensive experiments demonstrating the scalability and capability emergence of our CircuitAR and the superior performance of the proposed circuit generation approach.

2. Preliminaries

2.1. Modeling Circuit as DAG

In this work, we model the circuit as a directed acyclic graph (DAG) (Brummayer & Biere, 2006), which facilitates graph autoregressive modeling. Specifically, each node in the DAG corresponds to a logic gate, such as AND, OR, NAND, or other gate types, while the directed edges represent the connections between these components.

2.2. Differentiable CircuitNN

As depicted in Figure 1, CircuitNN (Google Deepmind, 2023) replaces traditional neural network layers with logic gates (e.g., NAND) as basic computational units, learning to synthesize circuits by optimizing logic correctness based on truth tables. During training, input connections of each gate are determined through learnable probability distributions, enabling adaptive circuit architecture modification. To enable gradient-based learning, CircuitNN transforms discrete logic operations into continuous, differentiable functions using NAND gates for simplicity. The NAND gate is logically complete, allowing the construction of any complex logic circuit. Its continuous relaxation can be defined as:

$$\text{NAND}(x, y) = 1 - x \cdot y, \text{ where } x, y \in [0, 1]. \quad (1)$$

Additionally, CircuitNN employs Gumbel-Softmax (Jang et al., 2016) for stochastic sampling of gate inputs. Through stochastic relaxation, gate and network outputs are no longer binary but take continuous values ranging from 0 to 1 instead. This end-to-end differentiability allows the model to learn gate input distributions using gradient descent. After training, the continuous, probabilistic circuit is converted back into a discrete logic circuit by selecting the most probable connections based on the learned probability distributions as shown in Figure 1.

3. Methodology

In this section, we first introduce CircuitVQ (Section 3.2), a model built upon the Circuit AutoEncoder framework (Section 3.1) and trained with the task of circuit reconstruction. Utilizing CircuitVQ as a tokenizer, we subsequently train

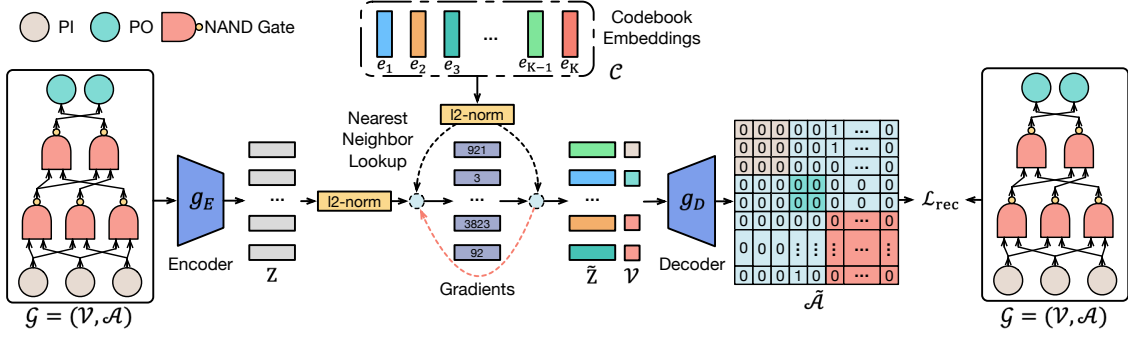


Figure 2. The training process of CircuitVQ, designed based on the circuit autoencoder and a vector quantizer.

CircuitAR (Section 3.3) with graph autoregressive modeling paradigm, which can generate preliminary circuit structures conditioned on a provided truth table. Finally, the initial circuit structure generated by CircuitAR serves as a guide for DAS (Section 3.4) to refine and generate circuits functionally equivalent to the given truth table.

3.1. Circuit AutoEncoder

Let $\mathcal{G} = (\mathcal{V}, \mathcal{A})$ represent a circuit, where \mathcal{V} denotes the set of N nodes, with each node $v_i \in \mathcal{V}$. Following the architecture of CircuitNN (Google Deepmind, 2023; Wang et al., 2024), each node v_i can be classified into one of three types: primary inputs (PIs), primary outputs (POs), and NAND gates, each labeled by $u_i \in \mathcal{U}, i \in \{1, 2, 3\}$ respectively. The adjacency matrix $\mathcal{A} \in \{0, 1\}^{N \times N}$ captures the connectivity between nodes, where $\mathcal{A}_{i,j} = 1$ indicates the presence of a directed edge from v_i to v_j .

In the circuit autoencoder framework, an encoder, denoted as g_E , encodes the circuit \mathcal{G} into a latent representation $\mathbf{Z} \in \mathbb{R}^{N \times d}$ with dimensionality d . The encoding process for a circuit can be formulated as:

$$\mathbf{Z} = g_E(\mathcal{V}, \mathcal{A}). \quad (2)$$

Simultaneously, a decoder g_D aims to reconstruct the original circuit \mathcal{G} from the latent representation \mathbf{Z} . Since node types can be directly derived from the truth table, the decoder is designed to focus on reconstructing the adjacency matrix \mathcal{A} , which can be formalized as follows:

$$\tilde{\mathcal{G}} = (\mathcal{V}, \tilde{\mathcal{A}}) = (\mathcal{V}, f(g_D(\mathbf{Z}, \mathcal{V}))), \quad (3)$$

where $\tilde{\mathcal{A}} \in \mathbb{R}^{N \times N}$ denotes the reconstructed adjacency matrix, obtained by decoding the latent representation \mathbf{Z} through g_D and applying a mapping function $f: \mathbb{R}^{N \times d} \rightarrow \mathbb{R}^{N \times N}$. Meanwhile, $\tilde{\mathcal{G}}$ represents the reconstructed graph. A robust encoder g_E capable of capturing fine-grained structural information is essential to facilitate the circuit reconstruction task. We incorporate the Graphormer (Ying et al., 2021) architecture into g_E . For the decoder g_D , we adopt a

simple Transformer-based (Dubey et al., 2024) architecture, as an overly powerful decoder could negatively impact the performance of the circuit tokenizer.

3.2. CircuitVQ

As mentioned in Section 3.1, we propose a circuit autoencoder architecture for the circuit reconstruction task. The outputs of g_E and the inputs of g_D are continuous. The circuit tokenizer is required to map the circuit to a sequence of discrete circuit tokens for masked autoregressive modeling illustrated in Section 3.3. Specifically, a circuit \mathcal{G} can be tokenized to $\mathbf{Y} = [y_1, y_2, \dots, y_N] \in \mathbb{R}^N$ using the circuit quantizer \mathcal{C} which contains K discrete codebook embeddings. Here, each token y_i belongs to the vocabulary set $\{1, 2, \dots, K\}$ of \mathcal{C} . Consequently, we develop a circuit tokenizer, CircuitVQ, based on the circuit autoencoder by integrating a circuit quantizer \mathcal{C} . As shown in Figure 2, the tokenizer comprises three components: a circuit encoder g_E , a circuit quantizer \mathcal{C} , and a circuit decoder g_D .

Firstly, g_E encodes the circuit into vector representations \mathbf{Z} . Subsequently, \mathcal{C} identifies the nearest neighbor in the codebook for $\mathbf{z}_i \in \mathbf{Z}$. Let $\{\mathbf{e}_1, \mathbf{e}_2, \dots, \mathbf{e}_K\}$ represent the codebook embeddings and $\mathbf{e}_K \in \mathbb{R}^d$. For the i -th node, the quantized code y_i is determined by:

$$y_i = \arg \min_j \|\ell_2(\mathbf{z}_i) - \ell_2(\mathbf{e}_j)\|_2, \quad (4)$$

where $j \in \{1, 2, \dots, K\}$ and ℓ_2 normalization is applied during the codebook lookup (Van Den Oord et al., 2017; Yu et al., 2021). This distance metric is equivalent to selecting codes based on cosine similarity. Consequently, the output of \mathcal{C} for each node representation \mathbf{z}_i can be calculated based on the given Equation (4):

$$\tilde{\mathbf{z}}_i = \mathcal{C}(\mathbf{z}_i) = \ell_2(\mathbf{e}_{y_i}), \text{ where } \tilde{\mathbf{z}}_i \in \tilde{\mathbf{Z}}. \quad (5)$$

After quantizing the circuit into discrete tokens, the ℓ_2 -normalized codebook embeddings $\tilde{\mathbf{Z}} = \{\tilde{\mathbf{z}}_i\}_{i=1}^N$ are fed to g_D . The output vectors $\tilde{\mathbf{X}} = \{\tilde{\mathbf{x}}_i\}_{i=1}^N = g_D(\tilde{\mathbf{Z}}, \mathcal{V})$ are used

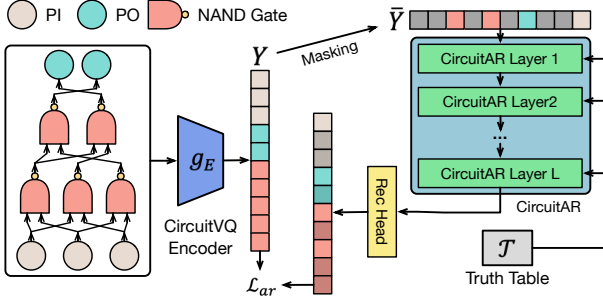


Figure 3. The training process of CircuitAR under the condition of the truth table, leveraging CircuitVQ as the tokenizer.

to reconstruct the original adjacency matrix \mathcal{A} of the circuit \mathcal{G} . Specifically, the reconstructed adjacency matrix $\tilde{\mathcal{A}}$ is derived from the output vectors $\tilde{\mathbf{X}}$ as follows:

$$\tilde{\mathcal{A}} = f(\tilde{\mathbf{X}}) = \sigma \left(f_1(\tilde{\mathbf{X}}) \cdot f_2(\tilde{\mathbf{X}})^T \right), \quad (6)$$

where both $f_1: \mathbb{R}^d \rightarrow \mathbb{R}^d$ and $f_2: \mathbb{R}^d \rightarrow \mathbb{R}^d$ are learnable projection functions, and $\sigma(x)$ denotes the sigmoid function. The training objective of the circuit reconstruction task is to minimize the binary cross-entropy loss between the reconstructed adjacency matrix $\tilde{\mathcal{A}}$ and the original adjacency matrix \mathcal{A} , which can be calculated as follows:

$$\mathcal{L}_{\text{rec}} = -\frac{1}{N^2} \sum_{i=1}^N \sum_{j=1}^N [\mathcal{A}_{ij} \log(\tilde{\mathcal{A}}_{ij}) + (1 - \mathcal{A}_{ij}) \log(1 - \tilde{\mathcal{A}}_{ij})]. \quad (7)$$

Given that the quantization process in Equation (4) is non-differentiable, gradients are directly copied from the decoder input to the encoder output during backpropagation, which enables the encoder to receive gradient updates. Intuitively, while the quantizer selects the nearest codebook embedding for each encoder output, the gradients of the codebook embeddings provide meaningful optimization directions for the encoder. Consequently, the overall training loss for CircuitVQ is defined as:

$$\mathcal{L}_{\text{vq}} = \mathcal{L}_{\text{rec}} + \|z - \text{sg}[e_{y_i}]\|_2^2 + \beta \cdot \|\text{sg}[z] - e_{y_i}\|_2^2 \quad (8)$$

where $\text{sg}[\cdot]$ stands for the stop-gradient operator which is an identity at the forward pass while having zero gradients during the backward pass and β denotes the hyperparameter for commitment loss (Van Den Oord et al., 2017).

Codebook utilization. A common issue in vector quantization training is codebook collapse, where only a small proportion of codes are actively utilized. To mitigate this problem, empirical strategies (Yu et al., 2021; Jang et al., 2016) are employed. Specifically, we compute the ℓ_2 -normalized distance to identify the nearest code while reducing the dimensionality of the codebook embedding space (Yu et al.,

Algorithm 1 Autoregressive Decoding of CircuitAR

Input: Masked tokens $\bar{\mathbf{Y}} = [\bar{y}_i]_{i=1}^N, \forall \bar{y}_i = m$, token length N , total iterations T .

Output: Predicted tokens $\tilde{\mathbf{Y}} = [\tilde{y}_i]_{i=1}^N \forall \tilde{y}_i \neq m$.

```

1: for  $t \leftarrow 0$  to  $T - 1$  do
2:   Initialize the number of masked tokens  $n$ ;
3:   Compute probabilities  $p(\bar{y}_i) \in \mathbb{R}^K$  for each  $\bar{y}_i \in \bar{\mathbf{Y}}$ ;
4:   Initialize  $\mathbf{S} \leftarrow [s_i]_{i=1}^N$ , where  $s_i = 0$ , and  $\tilde{\mathbf{Y}} \leftarrow \bar{\mathbf{Y}}$ ;
5:   for  $i \leftarrow 1$  to  $N$  do
6:     if  $\bar{y}_i = m$  then
7:       Sample a token  $o_i \in \{1, \dots, K\}$  from  $p(\bar{y}_i)$ ;
8:        $s_i \leftarrow p(\bar{y}_i)[o_i]$  and  $\tilde{y}_i \leftarrow o_i$ ;
9:     else
10:       $s_i \leftarrow 1$ ;
11:    end if
12:  end for
13:  for  $i \leftarrow 1$  to  $N$  and  $\bar{y}_i \neq m$  do
14:     $r \leftarrow \text{sorted}(\mathbf{S})[n]$ ; // Select the  $n$ -th highest score from the sorted  $\mathbf{S}$  in descending order
15:     $\tilde{y}_i \leftarrow \begin{cases} \tilde{y}_i, & \text{if } s_i < r, \\ \bar{y}_i, & \text{otherwise;} \end{cases}$ 
16:  end for
17:   $\tilde{\mathbf{Y}} \leftarrow \tilde{\mathbf{Y}}$ ;
18: end for
    
```

2021). These low-dimensional codebook embeddings are subsequently mapped back to a higher-dimensional space before being passed to the decoder. Furthermore, we leverage the Gumbel-Softmax trick (Jang et al., 2016) to enable smoother token selection during training, ensuring that a broader range of tokens in the codebook are actively trained, thereby improving the overall utilization of the codebook.

3.3. CircuitAR

After completing the CircuitVQ training, we train CircuitAR using a graph autoregressive modeling paradigm as shown in Figure 3, where CircuitVQ functions as the tokenizer. Let $\mathbf{Y} = [y_i]_{i=1}^N$ represent the discrete latent tokens of the input circuit \mathcal{G} , tokenized by CircuitVQ. During the masked autoregressive training process, we sample a subset of nodes $\mathcal{V}_s \subset \mathcal{V}$ and replace them with a special mask token m . For the masked \mathbf{Y} , the latent token \bar{y}_i is defined as:

$$\bar{y}_i = \begin{cases} y_i, & \text{if } v_i \notin \mathcal{V}_s; \\ m, & \text{if } v_i \in \mathcal{V}_s. \end{cases} \quad (9)$$

Following Chang et al. (2022) and Li et al. (2024a), we employ a cosine mask scheduling function $\gamma(r) = \cos(0.5\pi r)$ in the sampling process. This involves uniformly sampling a ratio r from the interval $[0, 1]$ and then selecting $\lceil \gamma(r) \cdot N \rceil$ tokens from \mathbf{Y} to mask uniformly. Let $\bar{\mathbf{Y}} = [\bar{y}_i]_{i=1}^N$ denote the output after applying the masking operation to

\mathbf{Y} . The masked sequence $\bar{\mathbf{Y}}$ is then fed into a multi-layer transformer with bidirectional attention to predict the probabilities $p(y_i|\bar{\mathbf{Y}}, \mathcal{T})$ for each $v_i \in \mathcal{V}_s$ under the condition of the truth table. The transformer is designed based on Llama models, each CircuitAR layer consists of a self-attention block, a cross-attention block and an FFN block. Specifically, the info of the truth table is conditioned by serving \mathcal{T} as the input key and value of the cross-attention block. The training loss for CircuitAR is defined as:

$$\mathcal{L}_{\text{ar}} = - \sum_{\mathcal{D}} \sum_{v_i \in \mathcal{V}_s} \log p(y_i|\bar{\mathbf{Y}}, \mathcal{T}), \quad (10)$$

where \mathcal{D} represents the set of training circuits.

Autoregressive decoding. We introduce a parallel decoding method, where tokens are generated in parallel. This approach is feasible due to the bidirectional self-attention mechanism of CircuitAR. At inference time, we begin with a blank canvas $\bar{\mathbf{Y}} = [m]^N$ and the decoding process of CircuitAR follows Algorithm 1. Specifically, the decoding algorithm generate a circuit in T steps. At each iteration, the model predicts all tokens simultaneously but retains only the most confident predictions following the cosine schedule (Chang et al., 2022; Li et al., 2024a). The remaining tokens are masked and re-predicted in the next iteration.

3.4. Differentiable Architecture Search

After completing the training process of CircuitAR, autoregressive decoding is performed based on the input truth table \mathcal{T} to generate preliminary circuit structures represented by the reconstructed adjacency matrix $\bar{\mathcal{A}}$. This matrix $\bar{\mathcal{A}}$ can serve as prior knowledge for DAS, enabling the generation of a precise circuit that is logically equivalent to \mathcal{T} .

DAG Search. The reconstructed adjacency matrix $\bar{\mathcal{A}}$ is a probability matrix that denotes the probabilities of connections between gates. However, $\bar{\mathcal{A}}$ may contain cycles. Identifying the optimal DAG with the highest edge probabilities is an NP-hard problem, we employ a greedy algorithm to obtain a suboptimal DAG. As illustrated in Algorithm 2, the algorithm initializes $\bar{\mathcal{A}} \in \mathbb{R}^{N \times N}$ with edge probabilities and enforces basic structural rules: PIs have no indegree, POs have no outdegree, and self-loops are prohibited in circuit designs. Following this initialization, a depth-first search (DFS) is conducted to detect cycles in $\bar{\mathcal{A}}$. If no cycles are found, $\bar{\mathcal{A}}$ is a valid DAG, and the algorithm terminates. If a cycle is detected, the edge with the lowest probability within the cycle is identified and removed by setting the corresponding edge in $\bar{\mathcal{A}}$ to 0. This process repeats iteratively until no cycles remain. This greedy approach ensures the derivation of a valid DAG $\bar{\mathcal{A}}$ that approximates the optimal structure while preserving the acyclic property necessary for circuit design. The resulting DAG serves as a foundation for further refinement in the DAS process, ultimately

Algorithm 2 DAG Search

Input: Adjacency matrix $\bar{\mathcal{A}} \in \mathbb{R}^{N \times N}$, PI node list Q_i , PO node list Q_o .

Output: Adjacency matrix $\bar{\mathcal{A}}$ of a valid DAG.

```

1: Initialize  $\bar{\mathcal{A}} \leftarrow \bar{\mathcal{A}}$ .
2: for each edge  $(i, j)$  in  $\bar{\mathcal{A}}$  ( $i \neq j$ ) do
3:    $\bar{\mathcal{A}}[i][j] \leftarrow 0$ .
4:   if  $i \notin Q_o$  and  $j \notin Q_i$  and  $\bar{\mathcal{A}}[i][j] > 0.5$  then
5:      $\bar{\mathcal{A}}[i][j] \leftarrow 1$ ;
6:   end if
7: end for
8: while True do
9:    $c \leftarrow \text{cycleDetect}(\bar{\mathcal{A}})$ ; // Detect a cycle using DFS
   and return the list of nodes forming the cycle.
10:  if  $\text{len}(c) = 0$  then
11:    break; // No cycles detected;  $\bar{\mathcal{A}}$  is a valid DAG.
12:  end if
13:  Initialize  $s \leftarrow \infty$ .
14:  for  $i \leftarrow 0$  to  $\text{len}(c) - 1$  do
15:     $j \leftarrow c[i]$  and  $k \leftarrow c[(i + 1) \bmod \text{len}(c)]$ ;
16:    if  $\bar{\mathcal{A}}[j][k] < s$  then
17:       $s \leftarrow \bar{\mathcal{A}}[j][k]$  and  $r \leftarrow (j, k)$ ;
18:    end if
19:  end for
20:   $\bar{\mathcal{A}}[r[0]][r[1]] \leftarrow 0$ ;
21: end while

```

generating a precise circuit that is logically equivalent to \mathcal{T} .

Initialization. After executing Algorithm 2, the adjacency matrix of a valid DAG $\bar{\mathcal{A}} \in \mathbb{R}^{N \times N}$ and its corresponding probability matrix $\hat{\mathcal{A}} = \bar{\mathcal{A}} \cdot \bar{\mathcal{A}}$, where $\hat{\mathcal{A}} \in \mathbb{R}^{N \times N}$, are obtained. Using $\bar{\mathcal{A}}$, we derive the hierarchical structure $H = \{h_1, h_2, \dots, h_l\}$, where h_l represents the node list of the l -th layer. The set H encapsulates the layer count l and the width information of each layer, which is used to initialize CircuitNN illustrated in Figure 1. For connection probabilities, since each node can only connect to nodes from preceding layers, we normalize the connection probabilities such that their summation equals 1. This yields the weights $w \in \mathbb{R}^{N_p}$ for possible connections, where N_p denotes the number of nodes in the previous layer. To ensure compatibility with the Softmax function applied in CircuitNN, we initialize the logits $\hat{w} \in \mathbb{R}^{N_p}$ such that the Softmax output matches the normalized connection probabilities. The logits are initialized as follows:

$$\hat{w} = \log(w + \epsilon) - \frac{1}{N_p} \sum_{i=1}^{N_p} \log(w_i + \epsilon), \quad (11)$$

where ϵ is a small constant for numerical stability. After initialization, the precise circuit structure is obtained through DAS, guided by the input truth table. Notably, if DAS converges to a local optimum, the weights of the least ini-

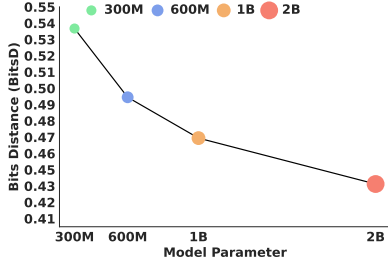


Figure 4. Scaling behavior of CircuitAR with different model parameters on circuit generation benchmark.

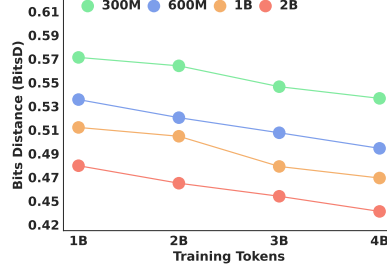


Figure 5. Training with more tokens improves BitsD for CircuitAR with different model parameters.

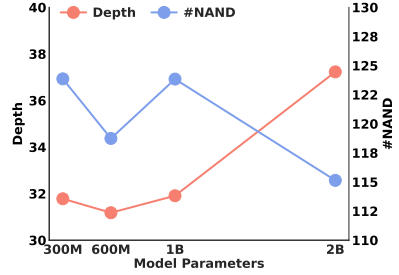


Figure 6. Emergent capability in generating complex circuit structures of our CircuitAR.

tialized nodes can be randomly selected and reinitialized using Equation (11) to facilitate further optimization.

3.5. Bits Distance

DAS introduces inherent randomness, complicating the evaluation of CircuitAR’s circuit generation capability using post-DAS metrics. To overcome this, we introduce Bits Distance (BitsD), a metric offering a more reliable assessment of CircuitAR’s conditional generation ability. BitsD quantifies the discrepancy between the outputs of an untrained CircuitNN, initialized via CircuitAR, and the labels from the truth table. It measures how well CircuitAR generates circuits conditioned on the truth table. Specifically, after initializing CircuitNN, we feed it with the truth table inputs and compute the mean absolute error (MAE) between the untrained CircuitNN outputs and the truth table labels. This MAE is defined as Bits Distance. A smaller BitsD indicates that the untrained CircuitNN is closer to the target circuit described by the truth table.

4. Experiments

4.1. Experiment Settings

Training Datasets. We generate training datasets with around 400k circuits (average 200 gates per circuit) from the open-source datasets (Bryan, 1985; Albrecht, 2005; Amarú et al., 2015). The training dataset construction details will be illustrated in Appendix B.

Data Augmentation. We provide more details about data augmentation in Appendix C and investigate the impact of idle of NAND gates in Appendix D.

Training Process. We provide more details about the training processes of CircuitVQ and CircuitAR in Appendix A.1 and Appendix A.2.

Baseline Selection. For baseline selection, we choose CircuitNN (Google Deepmind, 2023) and T-Net (Wang et al., 2024) due to their state-of-the-art (SOTA) performance in

circuit generation guided by truth tables. Additionally, several other studies (Tsaras et al., 2024; Li et al., 2024b; Zhou et al., 2024) have explored circuit generation using different paradigms. We discuss these approaches in Section 5, as they diverge from the DAS paradigm employed in this work.

Evaluation. To validate the effectiveness of our CircuitAR models, we conduct evaluations using circuits from the IWLS competition (Mishchenko et al., 2022), which include five distinct function categories: random, basic functions, Espresso (Rudell, 1985), arithmetic functions, and LogicNets (Umuroglu et al., 2020). Random circuits consist of random and decomposable Boolean functions, basic functions include majority functions and binary sorters, and arithmetic functions involve arithmetic circuits with permuted inputs and dropped outputs. Furthermore, we evaluate the BitsD for CircuitAR models with different sizes to assess their conditional circuit generation capability. This evaluation is performed on our circuit generation benchmark with 1000 circuits separate from the training dataset.

4.2. Scalability and Emergent Capability

To analyze CircuitAR’s scaling behavior, we perform experiments along two primary dimensions: parameter scaling (Figure 4) and data scaling (Figure 5). Our results reveal distinct performance patterns quantified through BitsD, demonstrating how these scaling axes influence performance. Additionally, we observe emergent capability in generating complex circuit structures of CircuitAR.

Parameter Scaling. As shown in Figure 4, increasing model capacity exhibits robust scaling laws. The 300M parameter model achieves 0.5317 BitsD, while scaling to 2B parameters yields 0.4362 BitsD. This progression follows a power-law relationship (Kaplan et al., 2020), where performance scales predictably with model size. Notably, marginal returns diminish at larger scales: the 0.3B→0.6B transition provides a 7.94% improvement versus 6.07% for 1B→2B, highlighting practical trade-offs between capacity and computational costs. These findings corroborate theo-

Table 1. Experiment results of circuit generation accuracy and DAS steps. Impr. is the percentage decrease in DAS steps.

Benchmark				CircuitNN		T-Net			CircuitAR-2B			
Category	IWLS	# PI	# PO	Acc.(%) \uparrow	Steps \downarrow	Acc.(%) \uparrow	Steps \downarrow	Impr.(%) \uparrow	Acc.(%) \uparrow	Steps \downarrow	Impr.(%) \uparrow	
Random	ex00	6	1	100	88715	100	85814	3.27	100	52023	41.36	
	ex01	6	1	100	64617	100	68686	-6.30	100	29636	54.14	
Basic Functions	ex11	7	1	100	104529	100	49354	52.78	100	47231	54.81	
	ex16	5	5	100	115150	100	121108	-5.17	100	45434	60.54	
	ex17	6	6	100	90584	100	57875	36.11	100	58548	35.66	
Expresso	ex38	8	7	100	86727	100	86105	0.71	100	74847	13.70	
	ex46	5	8	100	75726	100	75603	0.16	100	26854	64.54	
Arithmetic Function	ex50	8	2	100	87954	100	65689	25.31	100	42729	51.42	
	ex53	8	2	100	92365	100	75140	18.65	100	68246	38.26	
LogicNet	ex92	10	3	100	220936	100	206941	6.33	100	134192	39.26	
Average				100	102730	100	88831	13.19	100	57974	45.37	

Table 2. Experiment results of circuit generation size. Impr. represents the percentage decrease in search space and used NAND gates.

Benchmark		CircuitNN		T-Net				CircuitAR-2B			
Category	IWLS	# NAND \downarrow		# NAND \downarrow		Impr.(%) \uparrow		# NAND \downarrow		Impr.(%) \uparrow	
		Search Space	Used	Search Space	Used	Search Space	Used	Search Space	Used	Search Space	Used
Random	ex00	700	58	400	68	42.86	-17.24	126	61	82.00	-5.17
	ex01	700	66	400	62	42.86	6.06	138	66	80.29	0.00
Basic Functions	ex11	300	52	180	52	40.00	0.00	98	45	67.33	13.46
	ex16	700	78	400	59	42.86	24.36	113	57	83.86	26.92
	ex17	800	109	500	98	37.50	10.09	196	95	75.50	12.84
Expresso	ex38	800	98	500	94	37.50	4.08	178	86	77.75	12.24
	ex46	800	77	500	78	37.50	-1.30	161	79	79.88	-2.60
Arithmetic Functions	ex50	300	59	180	56	40.00	5.09	77	48	74.33	18.64
	ex53	1000	118	600	116	40.00	1.70	185	111	81.50	5.93
LogicNet	ex92	1000	99	600	90	40.00	9.09	168	86	83.20	13.13
Average		710	81.40	426	77.30	40.11	4.19	144	73.40	78.56	9.54

retical expectations (Thomas & Joy, 2006), confirming that larger models compress logical information more efficiently.

Data Scaling. Figure 5 illustrates consistent performance gains with increased training tokens across all sizes. For the 2B model, BitsD improves by 8.13% (0.4748 \rightarrow 0.4362) when scaling from 1B to 4B tokens. Moreover, larger models exhibit superior data efficiency. Specifically, the 2B model achieves better performance (0.4362 BitsD) with 4B tokens than the 1B model (0.4644 BitsD), emphasizing the interplay between model capacity and training scale.

Emergent Capability. Figure 6 highlights CircuitAR’s emergent capability in generating complex circuit structures. A clear phase transition is observed at the 2B parameter threshold, where circuit depth increases significantly compared to the 1B model, indicating an emergent capacity for handling structural complexity. Moreover, an inverse correlation between model scale and NAND gate count reveals an efficiency paradigm. While models ranging from 300M to 1B parameters maintain similar component counts, the 2B model achieves a reduction in NAND gates despite its increased depth, suggesting enhanced topological op-

timization capabilities at scale. This emergent behavior demonstrates that increasing model parameters can enhance structural efficiency in circuit generation.

4.3. SOTA Circuit Generation

Given the superior performance of CircuitAR-2B, as demonstrated in Section 4.2, we employ it to generate preliminary circuit structures conditioned on truth tables, which are subsequently refined using DAS. Detailed experimental results are presented in Table 1 and Table 2.

Efficiency. As illustrated in Table 1, CircuitAR-2B achieves a 45.37% average improvement in optimization steps compared to CircuitNN, while maintaining 100% accuracy according to the provided truth tables. This performance significantly surpasses T-Net’s 13.19% improvement. The substantial reduction in optimization steps indicates that the preliminary circuit structures generated by CircuitAR-2B effectively prune the search space without compromising the quality of DAS.

Effectiveness. Table 2 demonstrates that CircuitAR-2B reduces NAND gate usage by an average of 9.54% compared

Table 3. Ablation study on the initialization process with edge probability generated by CircuitAR-2B.

Benchmark		CircuitAR-2B w/o init		CircuitAR-2B	
Category	IWLS	Acc.(%) \uparrow	Steps \downarrow	Acc.(%) \uparrow	Steps \downarrow
Random	ex00	100	72364	100	52023
	ex01	100	40528	100	29636
Basic Functions	ex11	100	64517	100	47231
	ex16	100	76066	100	45434
	ex17	100	88609	100	58548
Espresso	ex38	100	99594	100	74847
	ex46	100	40892	100	26854
Arithmetic Function	ex50	100	69958	100	42729
	ex53	100	89627	100	68246
LogicNet	ex92	100	162651	100	134192
Average		100	80481	100	57974

to CircuitNN, while simultaneously reducing the search space by 78.56%. Notably, for both basic functions (e.g., ex16, with a 26.92% reduction) and complex benchmarks (e.g., ex92, with a 13.13% reduction), our method exhibits superior hardware resource utilization compared to the baseline approaches. This dual improvement in search space compression and circuit compactness underscores the effectiveness of the preliminary circuit structures generated by our CircuitAR-2B under the condition of the truth tables.

Critically, the 100% accuracy across all benchmarks confirms that our method maintains functional correctness while achieving these efficiency gains. These results validate our hypothesis that integrating learned structural priors with CircuitAR enables more sample-efficient circuit generation compared to basic CircuitNN (Google Deepmind, 2023) and template-driven (Wang et al., 2024) DAS approaches.

4.4. Ablation Study

We conducted an ablation study to evaluate the effectiveness of the probability matrix \hat{A} generated by CircuitAR-2B. As summarized in Table 3, the experiment results reveal that both variants achieve perfect accuracy (100%) across all benchmarks, suggesting that the initialization process does not impair the ability to generate functionally equivalent circuits. The primary distinction lies in the efficiency of the search process, quantified by the number of search steps. Table 3 underscores the significance of the initialization process, demonstrating that our CircuitAR models can produce high-quality preliminary circuit structures, which can guide the subsequent DAS process effectively.

5. Related Works

5.1. Autoregressive Modeling

The autoregressive modeling paradigm (OpenAI, 2023; Tian et al., 2024) has been widely adopted for generation tasks

in language and vision domains. Built on the transformer architecture, autoregressive models are commonly implemented using causal attention mechanisms in language domains (OpenAI, 2023), which process data sequentially. However, information does not inherently require sequential processing in vision and graph generation tasks. To address this, researchers have employed bidirectional attention mechanisms for autoregressive modeling (Li et al., 2024a; Tian et al., 2024; Chang et al., 2022; Li et al., 2023b). This approach predicts the next token based on previously predicted tokens while allowing unrestricted communication between tokens, thereby relaxing the sequential constraints of traditional autoregressive methods. In this paper, we adopt masked autoregressive modeling for circuit generation, leveraging its ability to provide a global perspective and enhance the modeling of complex dependencies.

5.2. Circuit Generation

In addition to the DAS-based approaches, researchers have also explored next-gate prediction techniques inspired by LLMs for circuit generation. Circuit Transformer (Li et al., 2024b) predicts the next logic gate using a depth-first traversal and equivalence-preserving decoding. SeaDAG (Zhou et al., 2024) employs a semi-autoregressive diffusion model for DAG generation, maintaining graph structure for precise control. ShortCircuit (Tsaras et al., 2024) uses a transformer to generate Boolean expressions from truth tables via next-token prediction. However, these methods are limited by their global view, restricting circuit size and failing to reduce the search space. In contrast, our approach uses global-view masked autoregressive decoding to generate circuits while ensuring logical equivalence and significantly reducing the search space during the DAS process.

6. Conclusion

In this paper, we propose a novel approach that integrates conditional generative models with DAS for circuit generation. Our framework begins with the design of CircuitVQ, a circuit tokenizer trained using a Circuit AutoEncoder. Building on this, we develop CircuitAR, a masked autoregressive model that utilizes CircuitVQ as its tokenizer. CircuitAR can generate preliminary circuit structures directly from truth tables, which are then refined by DAS to produce functionally equivalent circuits. The scalability and capability emergence of CircuitAR highlights the potential of masked autoregressive modeling for circuit generation tasks, akin to the success of large models in language and vision domains. Extensive experiments demonstrate the superior performance of our method, underscoring its efficiency and effectiveness. This work bridges the gap between probabilistic generative models and precise circuit generation, offering a robust and automated solution for logic synthesis.

Impact Statement

This paper presents work whose goal is to advance the field of Machine Learning. There are many potential societal consequences of our work, none which we feel must be specifically highlighted here.

References

- Abramson, J., Adler, J., Dunger, J., Evans, R., Green, T., Pritzel, A., Ronneberger, O., Willmore, L., Ballard, A. J., Bambrick, J., et al. Accurate Structure Prediction of Biomolecular Interactions with AlphaFold 3. *Nature*, pp. 1–3, 2024.
- Albrecht, C. IWLS 2005 Benchmarks. In *IEEE/ACM International Workshop on Logic Synthesis*, 2005.
- Amarú, L., Gaillardon, P.-E., and De Micheli, G. The EPFL Combinational Benchmark Suite. In *IEEE/ACM International Workshop on Logic Synthesis*, 2015.
- Brayton, R. and Mishchenko, A. ABC: An Academic Industrial-Strength Verification Tool. In *Computer Aided Verification: 22nd International Conference, CAV 2010, Edinburgh, UK, July 15-19, 2010. Proceedings 22*, pp. 24–40. Springer, 2010.
- Brummayer, R. and Biere, A. Local Two-Level and-Inverter Graph Minimization Without Blowup. *Proc. MEMICS*, 6:32–38, 2006.
- Bryan, D. The ISCAS’85 Benchmark Circuits and Netlist Format. *North Carolina State University*, 1985.
- Chang, H., Zhang, H., Jiang, L., Liu, C., and Freeman, W. T. MaskGIT: Masked generative image transformer. In *IEEE Conference on Computer Vision and Pattern Recognition (CVPR)*, 2022.
- Chu, X., Wang, X., Zhang, B., Lu, S., Wei, X., and Yan, J. DARTS-: Robustly stepping out of performance collapse without indicators. *arXiv preprint arXiv:2009.01027*, 2020.
- Dubey, A., Jauhri, A., Pandey, A., Kadian, A., Al-Dahle, A., Letman, A., Mathur, A., Schelten, A., Yang, A., Fan, A., et al. The llama 3 herd of models. *arXiv preprint arXiv:2407.21783*, 2024.
- Esser, P., Kulal, S., Blattmann, A., Entezari, R., Müller, J., Saini, H., Levi, Y., Lorenz, D., Sauer, A., Boesel, F., et al. Scaling Rectified Flow Transformers for High-Resolution Omage Synthesis. URL <https://arxiv.org/abs/2403.03206>, 2, 2024.
- Google Deepmind. Optimizing Computer Systems with More Generalized AI Tools. <https://deepmind.google/discover/blog/>, 2023.
- Hachtel, G. D. and Somenzi, F. *Logic Synthesis and Verification Algorithms*. Springer Science & Business Media, 2005.
- Hou, Z., Liu, X., Cen, Y., Dong, Y., Yang, H., Wang, C., and Tang, J. GraphMAE: Self-Supervised Masked Graph AutoEncoders. In *ACM International Conference on Knowledge Discovery and Data Mining (KDD)*, pp. 594–604, 2022.
- Jang, E., Gu, S., and Poole, B. Categorical Reparameterization with Gumbel-Softmax. *arXiv preprint arXiv:1611.01144*, 2016.
- Kaplan, J., McCandlish, S., Henighan, T., Brown, T. B., Chess, B., Child, R., Gray, S., Radford, A., Wu, J., and Amodei, D. Scaling laws for neural language models. *arXiv preprint arXiv:2001.08361*, 2020.
- Li, J., Wu, R., Sun, W., Chen, L., Tian, S., Zhu, L., Meng, C., Zheng, Z., and Wang, W. What’s Behind the Mask: Understanding Masked Graph Modeling for Graph Autoencoders. In *ACM International Conference on Knowledge Discovery and Data Mining (KDD)*, pp. 1268–1279, 2023a.
- Li, T., Chang, H., Mishra, S., Zhang, H., Katabi, D., and Krishnan, D. MAGE: Masked generative encoder to unify representation learning and image synthesis. In *IEEE Conference on Computer Vision and Pattern Recognition (CVPR)*, 2023b.
- Li, T., Tian, Y., Li, H., Deng, M., and He, K. Autoregressive Image Generation without Vector Quantization. *arXiv preprint arXiv:2406.11838*, 2024a.
- Li, X., Li, X., Chen, L., Zhang, X., Yuan, M., and Wang, J. Circuit Transformer: End-to-end Circuit Design by Predicting the Next Gate. *arXiv preprint arXiv:2403.13838*, 2024b.
- Liu, H., Simonyan, K., and Yang, Y. DARTS: Differentiable Architecture Search. *arXiv preprint arXiv:1806.09055*, 2018.
- Mishchenko, A., Chatterjee, S., Amarú, L., Testa, E., and Lau Neto, W. IWLS 2022 Programming Contest. <https://github.com/alanminko/iwls2022-ls-contest/>, 2022.
- OpenAI. GPT-4 Technical Report. *arXiv preprint arXiv:2303.08774*, 2023.
- Rudell, R. Espresso-mv: Algorithms for multiple-valued logic minimization. In *Proceedings of IEEE Custom Integrated Circuit Conference*, pp. 230–234, 1985.
- Thomas, M. and Joy, A. T. *Elements of information theory*. Wiley-Interscience, 2006.

- Tian, K., Jiang, Y., Yuan, Z., Peng, B., and Wang, L. Visual autoregressive modeling: Scalable image generation via next-scale prediction. In *Annual Conference on Neural Information Processing Systems (NIPS)*, 2024.
- Tsaras, D., Grosnit, A., Chen, L., Xie, Z., Bou-Ammar, H., and Yuan, M. ShortCircuit: AlphaZero-Driven Circuit Design. *arXiv preprint arXiv:2408.09858*, 2024.
- Umuroglu, Y., Akhauri, Y., Fraser, N. J., and Blott, M. Logicnets: Co-designed neural networks and circuits for extreme-throughput applications. In *International Conference on Field-Programmable Logic and Applications (FPL)*, pp. 291–297. IEEE, 2020.
- Van Den Oord, A., Vinyals, O., et al. Neural Discrete Representation Learning. In *Annual Conference on Neural Information Processing Systems (NIPS)*, 2017.
- Wang, Z., Wang, J., Yang, Q., Bai, Y., Li, X., Chen, L., Jianye, H., Yuan, M., Li, B., Zhang, Y., et al. Towards Next-Generation Logic Synthesis: A Scalable Neural Circuit Generation Framework. In *Annual Conference on Neural Information Processing Systems (NIPS)*, 2024.
- Wolf, C., Glaser, J., and Kepler, J. Yosys-a free verilog synthesis suite. In *Proceedings of the 21st Austrian Workshop on Microelectronics (Austrochip)*, volume 97, 2013.
- Wu, H., Zheng, H., Pu, Y., and Yu, B. Circuit Representation Learning with Masked Gate Modeling and Verilog-AIG Alignment. In *International Conference on Learning Representations (ICLR)*, 2025. URL <https://openreview.net/forum?id=US9k5TXVLZ>.
- Ying, C., Cai, T., Luo, S., Zheng, S., Ke, G., He, D., Shen, Y., and Liu, T.-Y. Do transformers really perform badly for graph representation? In *Annual Conference on Neural Information Processing Systems (NIPS)*, 2021.
- Yu, J., Li, X., Koh, J. Y., Zhang, H., Pang, R., Qin, J., Ku, A., Xu, Y., Baldrige, J., and Wu, Y. Vector-Quantized Image Modeling with Improved VQGAN. *arXiv preprint arXiv:2110.04627*, 2021.
- Zhou, X., Li, X., Lian, Y., Wang, Y., Chen, L., Yuan, M., Hao, J., Chen, G., and Heng, P. A. SeaDAG: Semi-autoregressive Diffusion for Conditional Directed Acyclic Graph Generation. *arXiv preprint arXiv:2410.16119*, 2024.

A. Implementation Details

A.1. CircuitVQ

The training process of CircuitVQ employs a linear learning rate schedule with the AdamW optimizer set at a learning rate of 2×10^{-4} , a weight decay of 0.1, and a batch size of 2048. The model is fine-tuned for 20 epochs on $8 \times A100$ GPUs with 80G memory each. Moreover, we use the Graphormer (Ying et al., 2021) as our CircuitVQ architecture as mentioned before. Specifically, CircuitVQ comprises 6 encoder layers and 1 decoder layer. The hidden dimension and FFN intermediate dimension are 1152 and 3072, respectively. Additionally, the multi-head attention mechanism employs 32 attention heads. For the vector quantizer component, the codebook dimensionality is set to 4 to improve the codebook utilization, and the codebook size is configured to 8192.

A.2. CircuitAR

The training process of CircuitAR employs a linear learning rate schedule with the AdamW optimizer set at a learning rate of 2×10^{-4} , a weight decay of 0.1, and a batch size of 4096. The model is fine-tuned for 20 epochs on $16 \times A100$ GPUs with 80G memory each. Moreover, we use the Transformer variant of Llama (Dubey et al., 2024) as our CircuitAR architecture as mentioned before. To form different model sizes, we vary the hidden dimension, FFN intermediate dimension, number of heads and number of layers. We present the details of our CircuitAR architecture configurations in Table 4. For the rest of the hyperparameters, we keep them the same as the standard Llama model.

Table 4. Model architecture configurations of CircuitAR.

	hidden dim	FFN dim	heads	layers
CircuitAR-300M	1280	3072	16	16
CircuitAR-600M	1536	4096	16	20
CircuitAR-1B	1800	6000	24	24
CircuitAR-2B	2048	8448	32	30

B. Training Datasets

This section presents a multi-output subcircuit extraction algorithm designed for generating training datasets. The algorithm processes circuits represented in the And Inverter Graph (AIG) format by iterating over each non-PI node as a pivot node. The extraction process consists of three key stages:

1. **Single-Output Subcircuit Extraction.** The algorithm extracts single-output subcircuits by analyzing the transitive fan-in of the pivot node. The transitive fan-in includes all nodes that influence the output of the pivot node, encompassing both direct predecessors and nodes that propagate signals to it. The extraction process employs a breath-first search (BFS) algorithm, constrained by a maximum input size, to ensure comprehensive coverage of relevant nodes associated with the pivot node.
2. **Multi-Output Subcircuit Expansion.** Single-output subcircuits are expanded into multi-output subcircuits through transitive fan-out exploration. The transitive fan-out comprises all nodes influenced by the pivot node, including immediate successors and downstream nodes reachable through signal propagation. This expansion captures the broader network of nodes that either influence or are influenced by the subcircuits of the pivot node.
3. **Truth Table Generation.** The algorithm computes truth tables for the extracted subcircuits to serve as training labels. Additionally, these truth tables help identify functionally equivalent subcircuits. Recognizing these equivalences is essential, as it can lead to data imbalance in the training set.

To mitigate data imbalance, a constraint is imposed, limiting each truth table to at most M distinct graph topologies. For truth tables with fewer than M representations, logic synthesis techniques (specifically rewriting algorithms) are applied to generate functionally equivalent subcircuits with distinct topologies. This approach ensures topological diversity while maintaining functional equivalence. Finally, the training datasets with around 400000 circuits (average 200 gates per circuit) are generated using circuits from the ISCAS’85 (Bryan, 1985), IWLS’05 (Albrecht, 2005), and EPFL (Amarú et al., 2015) benchmarks. The maximum input size is set to 16, and M is set to 5 during the generation process.

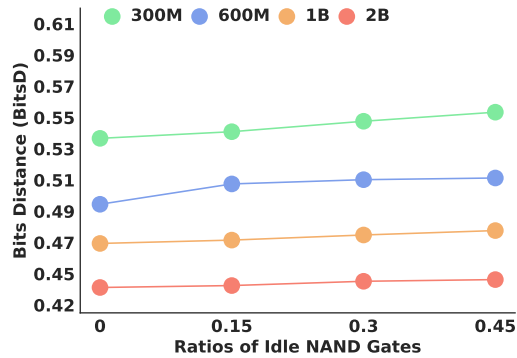


Figure 7. The impact of idle NAND gates on BitsD for CircuitAR with different ratios of isolated NAND gates.

C. Data Augmentation

Following dataset generation, we identified that the data volume was still insufficient. To address this limitation, we implemented data augmentation techniques. Leveraging the topological invariance of graphs, we randomly shuffled the order of graph nodes, as this operation does not alter the underlying structure of the circuit. Furthermore, since inserting idle nodes preserves the circuit structure, we randomly introduced idle nodes into the graphs. The proportion of idle nodes is randomly selected ranging from 0% to 80%. Moreover, incorporating idle nodes enables CircuitAR to identify which nodes can remain inactive for a fixed number of nodes. This allows CircuitAR to generate circuits logically equivalent to the truth table while utilizing fewer graph nodes. This strategy can improve CircuitAR’s efficiency and enhance its generalizability.

D. Idle NAND Gates

As illustrated in Figure 7, all model variants exhibit a gradual decline in BitsD as the proportion of isolated gates increases from 0% to 45%. Larger models (2B parameters), demonstrate significantly greater robustness, maintaining BitsD values within a narrow range (0.4362 to 0.4413) across varying isolation ratios. In contrast, smaller models (300M parameters) show a more pronounced degradation, with BitsD increasing from 0.5317 to 0.5484 under the same conditions. This disparity highlights the enhanced ability of larger models to efficiently utilize NAND gates for implementing the same truth table. The consistently low BitsD observed in the 2B model (0.4412 at 45% idle ratios) underscores its practical utility in predefining search spaces for DAS, offering a notable advantage over smaller models.